Advances in Radiation Oncology (2021) **6**, 100666

advances
in radiation oncology

www.advancesradonc.org

Scientific Article

Investigating the SPECT Dose-Function Metrics Associated With Radiation-Induced Lung Toxicity Risk in Patients With Non-small Cell Lung Cancer Undergoing Radiation Therapy

Daniel R. Owen, BS,[a,*] Yilun Sun, PhD,[a,b] Philip S. Boonstra, PhD,[b] Matthew McFarlane, MD, PhD,[a] Benjamin L. Viglianti, MD, PhD,[c,d] James M. Balter, PhD,[a] Issam El Naqa, PhD,[a] Matthew J. Schipper, PhD,[b] Caitlin A. Schonewolf, MD,[a] Randall K. Ten Haken, PhD,[a] Feng-Ming S. Kong, MD, PhD,[e,f] Shruti Jolly, MD,[a] and Martha M. Matuszak, PhD[a]

[a]Department of Radiation Oncology, University of Michigan, Ann Arbor, Michigan; [b]Department of Biostatistics, University of Michigan, Ann Arbor, Michigan; [c]Department of Radiology, University of Michigan, Ann Arbor, Michigan; [d]Veterans Administration, Nuclear Medicine Service, Ann Arbor Michigan; [e]Hong Kong University Shenzhen Hospital and Queen Mary Hospital, Hong Kong University Li Ka Shing Medical School, Department of Clinical Oncology, Hong Kong; and [f]Department of Radiation Oncology, Case Western Reserve University, Cleveland, Ohio

Received 20 July 2020; revised 18 December 2020; accepted 22 January 2021

Purpose: Dose to normal lung has commonly been linked with radiation-induced lung toxicity (RILT) risk, but incorporating functional lung metrics in treatment planning may help further optimize dose delivery and reduce RILT incidence. The purpose of this study was to investigate the impact of the dose delivered to functional lung regions by analyzing perfusion (Q), ventilation (V), and combined V/Q single-photon-emission computed tomography (SPECT) dose-function metrics with regard to RILT risk in patients with non-small cell lung cancer (NSCLC) patients who received radiation therapy (RT).

Methods and Materials: SPECT images acquired from 88 patients with locally advanced NSCLC before undergoing conventionally fractionated RT were retrospectively analyzed. Dose was converted to the nominal dose equivalent per 2 Gy fraction, and SPECT intensities were normalized. Regional lung segments were defined, and the average dose delivered to each lung region was quantified. Three functional categorizations were defined to represent low-, normal-, and high-functioning lungs. The percent of functional lung category receiving $\geq$20 Gy and mean functional intensity receiving $\geq$20 Gy (iV_{20}) were calculated. RILT was defined as grade 2+ radiation pneumonitis and/or clinical radiation fibrosis. A logistic regression was used to evaluate the association between dose-function metrics and risk of RILT.

Sources of support: This work was supported in part by R01-CA142840 (Kong), P30-CA046592 (Lawrence), KQTD20180411185028798 (Kong), and P01-CA059872 (Ten Haken/Lawrence).

Disclosures: Drs Owen, Sun, Boonstra, McFarlane, Viglianti, Schonewolf, and Balter have nothing to disclose. Dr El Naqa reports grants from the National Institutes of Health (NIH), Endectra LLC, and Resero AI LLC outside of the submitted work. Dr Schipper reports personal fees from Innovative Analytics outside of the submitted work. Dr Ten Haken reports grants from the NIH during the conduct of the study and nonfinancial support from Varian Medical Systems outside of the submitted work. Dr Kong reports grants from NIH/National Cancer Institute during the conduct of the study and grants and personal fees from Varian Medical Systems outside the submitted work. Dr Jolly reports personal fees from Varian Medical Systems outside of the submitted work. Dr Matuszak reports grants from the NIH during the conduct of the study and grants and other support from Varian Medical Systems outside of the submitted work.

* Corresponding author: Daniel R. Owen BS; E-mail: rockyo@umich.edu

https://doi.org/10.1016/j.adro.2021.100666

Results: By analyzing V/Q normalized intensities and functional distributions across the population, a wide range in functional capability (especially in the ipsilateral lung) was observed in patients with NSCLC before RT. Through multivariable regression models, global lung average dose to the lower lung was found to be significantly associated with RILT, and Q and V iV_{20} were correlated with RILT when using ipsilateral lung metrics. Through a receiver operating characteristic analysis, combined V/Q low-function receiving $\geq$20 Gy (low-functioning V/Q_{20}) in the ipsilateral lung was found to be the best predictor (area under the curce: 0.79) of RILT risk.
Conclusions: Irradiation of the inferior lung appears to be a locational sensitivity for RILT risk. The multivariable correlation between ipsilateral lung iV_{20} and RILT, as well as the association of low-functioning V/Q_{20} and RILT, suggest that irradiating low-functioning regions in the lung may lead to higher toxicity rates.

Introduction

Radiation-induced lung toxicity (RILT) is a common side effect in patients with non-small cell lung cancer (NSCLC) undergoing radiation therapy (RT) owing to the high prescription doses and large volumes of normal lung incident in the radiation field. Local failure remains a significant hazard in the management of NSCLC, but increasing tumor control while limiting RILT risk has long been a goal. In a secondary analysis of the Radiation Therapy Oncology Group 0617 randomized trial, the use of intensity modulated RT compared with 3-dimensional conformal RT planning was associated with lower rates of severe radiation pneumonitis (RP), suggesting that dose modulation can help to reduce toxicity.[1] As such, ongoing clinical trials, including Radiation Therapy Oncology Group study 1106, aim to improve local control through the use of positron emission tomography (PET) adaptive RT planning to specifically increase the dose to the actively growing tumor.[2]

Another strategy hypothesized to improve the therapeutic ratio is to preferentially limit the dose to functional lung to reduce the risk of RILT. This has been an area of investigation since the early 1990s, when studies from the Netherlands Cancer Institute[3] and Duke University[4] first investigated the use of functional lung imaging in RT planning. Both Boersma et al.[5] and Marks et al.[6] successfully used single-photon-emission computed tomography (SPECT) to quantify functional lung changes after RT, which motivated the potential to inversely incorporate perfusion (Q) and/or ventilation (V) metrics in RT planning.[7] In 2002, Seppenwoolde et al. theorized that RT plans could be optimized to maximize lung function after treatment by sparing well-perfused lung tissue,[8] which has formed the basis for functional-avoidance RT planning in patients with lung cancer. However, this recommendation was based on the inability for bullous lungs (ie, regions of poor Q and V) to reperfuse after RT and was not based on the study of its direct impact to patient outcome[9]. Although functional-avoidance may play a vital role in the treatment of some patients, an enhanced understanding of dose-function metrics associated with RILT is needed to ensure optimal patient-specific dose delivery.

Currently, most RT plans designed for patients with NSCLC are developed solely to limit physical dose metrics, such as mean lung dose and the volume of the lung receiving >20 Gy (V_{20}). These volumetric dosimetrics treat all lungs as functionally equivalent, but in practice there is wide variation in the functional distribution, both within a patient's lungs as well as between patients. Recently, computed tomography (CT)-based functional imaging has gained interest as a possible tool for functional lung mapping due to its ability to quantify ventilation-based metrics and its wide availability in the clinic. Vinogradskiy et al. observed extensive functional defects in patients with stage III NSCLC, and demonstrated functional-avoidance RT techniques using 4-dimensional CT ventilation maps.[10,11] Based on this research[12] and various other studies,[13,14] functional-avoidance clinical trials are underway at numerous institutions.[15–18]

In theory, functional imaging allows for personalized RT planning that can minimize damage, and ultimately reduce the risk of RILT. Despite this potential, there is little clinical data to validate its effective approach to reducing toxicity, and specifically that shifting doses from high-functioning (HF) into low-functioning (LF) regions in patients with heterogeneous lung function reduces the incidence or severity of RILT. The purpose of this study was to investigate the utility of functional lung images in RT planning by analyzing the correlation between V/Q SPECT-based dose-function metrics and the incidence of RILT. Specifically, we defined functional lung categorizations based on Q, V, and combined V/Q, and quantified the delivered dose to these various functional lung regions in an attempt to identify dose-function metrics associated with grade 2+ RILT incidence. Through this study, we aim to better understand the implications of redistributing dose in the lung, and identify functional targets that may be used to mitigate RILT incidence through functional-guided RT planning.

Methods and Materials

Patient cohort

A total of 88 patients with NSCLC treated with conventionally fractionated RT, with (n = 76) and without (n = 13) concurrent chemotherapy, from 2 separate institutional review board–approved studies (NCT00603057: n = 58, treated 2007-2013; NCT02492867: n = 30, treated 2015-2019) were retrospectively analyzed. The prescription dose in both cohorts was typically 60 to 74 Gy over 30 fractions. However, the latter cohort was primarily treated with volumetric modulated arc therapy, as opposed to 3-dimensional conformal RT, and functional-avoidance RT planning and replanning (ie, adaptive RT at midtreatment) was implemented to limit the dose to above-average V/Q SPECT functional intensity. In this study, RILT was defined as grade 2+ RP and/or grade 2+ clinical pulmonary fibrosis. RP and pulmonary fibrosis were diagnosed and graded prospectively according to a prespecified system,[19] with a grading scale consistent with that of the Common Terminology Criteria for Adverse Events, version 3.0, and the maximal grade was reported.[20] These pathologies are often considered distinct clinical processes, but RILT encompasses the primary dose-limiting pulmonary complications that impact patient survival and quality of life, and some evidence suggests that these toxicities may be linked.[21,22]

Data processing

V/Q SPECT/CT scans (voxel size: 3. 5 × 3.5 × 2 mm) were obtained from each patient (Symbia T6, Siemens Medical Solutions, Malvern, PA) before RT, with the patient supine and immobilized, using a standard thorax support device. Each patient was imaged first for pulmonary V by inhaling aerosolized ^{99m}Tc-diethylenetriaminepentaacetic from an 1850 MBq reservoir, and subsequently for pulmonary Q after an intravenous injection of 185 MBq of ^{99m}Tc-labeled macroaggregated albumin particles. Each SPECT scan was rigidly registered to the treatment planning CT using an alignment tool embedded in a commercial treatment planning system (Eclipse, Varian Medical Systems, Palo Alto, CA). Through the application programming interface within this treatment planning system, a novel program (C#) was implemented to process and analyze the spatially aligned dose-function data. Saturation artifacts were cleansed from the SPECT images by removing any voxel with functional intensity >3 standard deviations above the mean of the normal-functioning (F) region. Raw SPECT intensities (f_i) were normalized to the average intensity in the low-dose (≤5 Gy), F region of the contralateral lung ($\mathbb{N}$), as shown in Equation 1, because this region was assumed to be stable against radiation-induced longitudinal functional changes.

$$\forall \textit{ voxels in the lungs} : f_i^{\mathbb{N}} = \frac{f_i}{\mathbb{N}} \textit{ where } \mathbb{N} = \sum_{i=1}^{N_{norm}} \frac{f_i}{N_{norm}} \quad (1)$$

where N_{norm} is the number of voxels in the contralateral lung that had functional intensity between 15% and 70% of the maximum intensity (ie, F) and received ≤5 Gy (ie, low-dose). This normalization was performed to equalize functional values such that a normalized functional intensity of 1.0 equates to the average intensity of normal-functioning lung for all patients. Normalized Q and V SPECT intensities were used as a direct surrogate for lung function, and dose values were converted to the nominal dose equivalent per 2 Gy fraction (EQD2) to biologically correct for fractionation of the RT dose (α/β = 2.5 Gy).[23]

Three functional categorizations were created to represent LF, F, and HF lungs. Each voxel with normalized functional intensity $f_i^{\mathbb{N}}$ was assigned a functional categorization based on the schema below:

$$\left\{ \begin{array}{l} LF \textit{ if } f_i^{\mathbb{N}} < 15\% \textit{ of } f_{maximum}^{\mathbb{N}} \\ F \textit{ if } 15\% \textit{ of } f_{maximum}^{\mathbb{N}} \le f_i^{\mathbb{N}} < 70\% \textit{ of } f_{maximum}^{\mathbb{N}} \\ HF \textit{ if } f_i^{\mathbb{N}} \ge 70\% \textit{ of } f_{maximum}^{\mathbb{N}} \end{array} \right\}$$

where $f_{maximum}^{\mathbb{N}}$ is the maximum normalized functional intensity in the lung. The functional categorization limits were chosen based on previous guidance,[9,24] and determined before any statistical modeling. An example image of the functional categorizations is shown in Figure E1. For this study, patients with <5% LF lungs were considered to have no functional defects.

Pretreatment dose-function metrics were calculated within the global, ipsilateral (ie, individual lung structure receiving the higher mean dose), and contralateral lungs using clinically defined lung contours, excluding the gross tumor volume and a 4 mm inner boundary (~voxel width) to reduce the partial volume effect. Regional lung segments were defined as follows: upper lung above the carina, lower lung below the inferior pulmonary vein, and middle lung between the two. The number of patients with primary tumor involvement in the given lung sextant, with grade 2+ RILT cases in parentheses, were as follows: right upper lung = 33 (2); right middle lung = 10 (2); right lower lung = 8 (4); left upper lung = 23 (4); left middle lung = 11 (2); and left lower lung = 3 (1). However, of note, there was also significant tumor involvement in the mediastinum for many of these cases. A summary of baseline patient characteristics and dose-function metrics in the various patient cohorts in this analysis are listed in Table E1.

Patient age, normal lung volume, and volumetric dosimetrics, including mean lung dose, volume of lung receiving ≥5 Gy (V_5), and V_{20}, were calculated for each

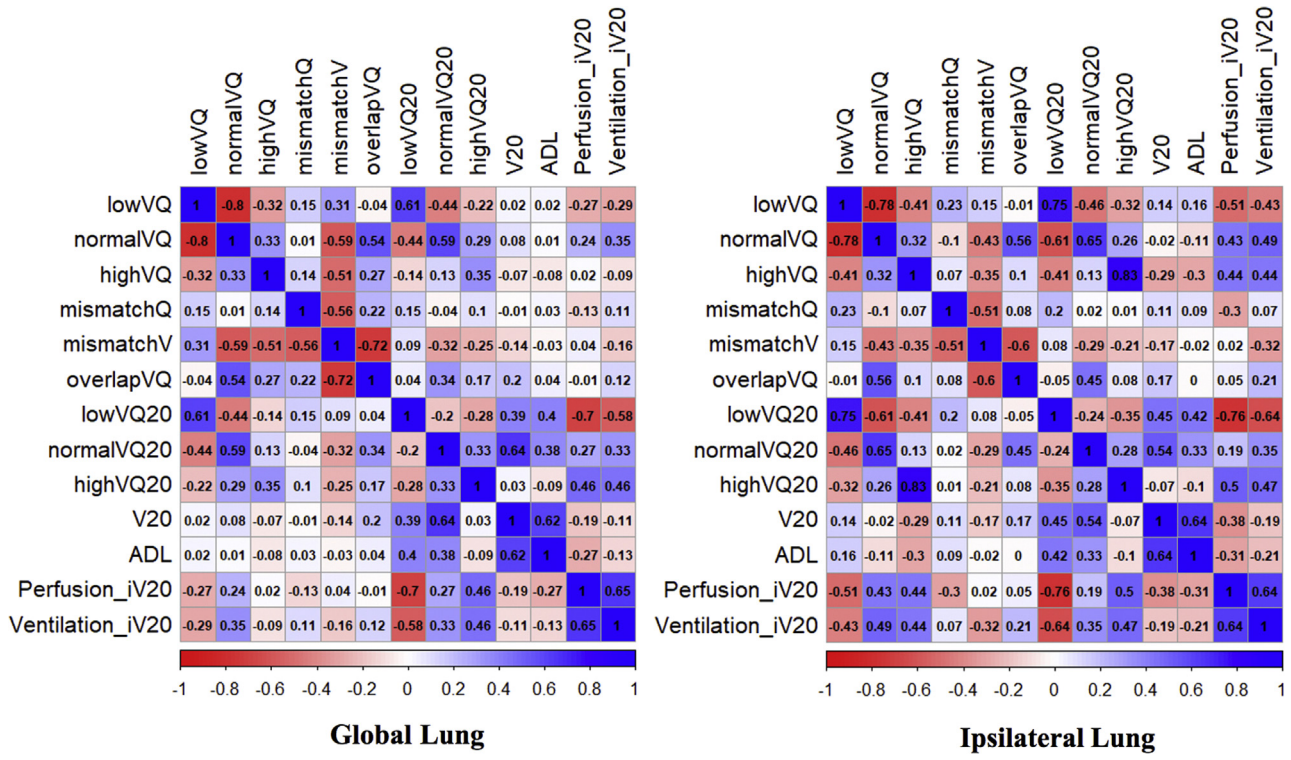

Figure 1 Bivariate spearman correlation coefficients

patient. The average dose to each regional lung segment was quantified. Functional metrics, including mean intensity, mean intensity in voxels receiving ≥5 Gy (iV_5), iV_{20}, and percent of functional lung category receiving ≥20 Gy ($LF_{20}/F_{20}/HF_{20}$) were calculated. The mean intensity receiving greater than dose d was calculated using Equation 2:

$$iVd = if\ d_i \geq d \rightarrow \sum_{i=1}^{N_d} \frac{f_i^{\mathbb{N}}}{N_d} \tag{2}$$

where d_i is the EQD2 dose in the i^{th} voxel and N_d is the total number of voxels receiving a dose greater than the threshold dose d. The percent of functional lung category F receiving threshold dose d was calculated as shown in Equation 3:

$$Fd = if\ f_i^{\mathbb{N}} \ni F\ \&\ d_i \geq d \rightarrow \frac{N_{F>d}}{N} \tag{3}$$

where $N_{F>d}$ is the number of voxels in functional category F that received at least dose d and N is the total number of voxels in the structure. The Fd metric was calculated in terms of Q, V, and combined V/Q (ie, both Q and V intensities were considered for the functional categorization of each voxel. For example, a given voxel must have both LF Q and LF V to be considered a combined V/Q LF voxel). A list of abbreviations is included in the supplementary table.

Statistical modeling

V, Q, and combined V/Q functional metrics were calculated in 88 patients. Spearman correlation coefficients were calculated for volumetric dosimetrics and combined V/Q functional metrics as shown in Figure 1. A paired t test was used to assess significant differences in metrics between patient cohorts. Patient, dose, and functional metrics were tested for their association with the incidence of grade 2+ RP or pulmonary fibrosis (ie, RILT) using the odds ratios (ORs) from univariate and multivariable logistic regression analyses. Normal lung volume, V_{20}, average dose to lower lung (ADL), and iV_{20} were chosen for inclusion in the multivariable model based on univariate association to represent patient, dose, location, and functional sensitivities that may independently influence RILT incidence. Receiver operating characteristic (ROC) curves were generated and area-under-the-curve (AUC) values were calculated using logistic regression models. The 95% confidence intervals (CIs) were calculated for the purpose of measuring uncertainty and assessing metric stability. A 5-fold cross-validation was used to minimize overly optimistic bias. For all analyses, 2-sided P-values of $< .05$ were considered statistically significant and values $< .1$ a marginal association. Analyses were performed using R (version 3.6.1) and MATLAB (version 9.4).

Results

This study combined data from 2 institutional review board–approved clinical trials (NCT00603057 & NCT02492867) in which V/Q SPECT images were obtained from 88 patients with NSCLC before undergoing RT. Patient characteristics and voxel-wise metrics quantifying volumetric dose, functional lung, and dose delivered to the functional lung for both patient cohorts are summarized in Table E1. The latter cohort was primarily treated with volumetric modulated arc therapy, as opposed to 3-dimensional conformal RT in the former cohort, which is reflected by the significantly higher V_5 and fV_5 values caused by the larger low-dose bath associated with modulated RT. Above-average Q and V were used as functional-avoidance priorities in the latter cohort, and yet no other metrics were found to significantly differ between the cohorts.

Individual patient and population-averaged (n = 88) Q and V functional distributions before RT are shown in Figure E2. For reference, a functional intensity of 1.0 is considered the average value of normal function, and a normal distribution around 1.0 is expected for a healthy individual. These normal distributions are largely exemplified by the 38 patients with <5% Q low function, as shown in Figure E3. As another reference, the population-average Q (V) LF and HF categorization thresholds, in absolute intensity, were 0.32 (0.38) and 1.49 (1.76), respectively. Mean Q and V intensities in various regions of the lung are depicted in Figure E4 to demonstrate the range of functional capability observed. Across the population, mean Q (V) intensity in the global lungs, ipsilateral lung, and contralateral lung were found to be 0.90 (0.87), 0.82 (0.81), and 0.96 (0.91), respectively. In patients exhibiting <5% LF, the mean global Q (n = 38) and V (n = 21) intensity were 0.96 and 0.95, respectively. On the contrary, 50 patients were found to have >5% Q LF and 67 patients were found to have >5% V LF, which corresponded to a global average Q and V of 0.86 and 0.84, respectively. In patients who incurred RILT (n = 15), the average Q and V intensity in the ipsilateral lung was found to be 0.68 and 0.66, respectively, signifying a large presence of functional defects in these patients. Additionally, for both Q and V, the population-averaged iV_{20} was less than the average functional intensity in the RILT cohort, demonstrating that a high dose was primarily funneled through below-average functioning lung in patients who incurred RILT.

Through a univariable logistic regression analysis, ipsilateral lung Q and V LF were significantly associated with RILT incidence, as shown in Table E2. Normal-functioning Q and V were also found to be associated with RILT, but inversely correlated, suggesting that patients with a less normal-functioning lung were at a higher risk. For both Q and V, the ipsilateral lung tended to exhibit a lower mean intensity and higher percent of LF than the contralateral lung. Ipsilateral lung volumetric dosimetrics (including V_{20} and mean dose) and dose-function metrics (including iV_{20} and LF_{20}) were also correlated with RILT on univariate analysis. Both iV_{20} (a continuous metric that quantifies average functional intensity delivered ≥20 Gy) and LF_{20} (percent of total volume that received ≥20 Gy to LF lung) correlations suggest that patients receiving more dose to the dysfunctional lung may be the most at risk for RILT.

The only contralateral lung metric associated with RILT was ADL. Although 65% of patients were found to have primary tumor involvement in the upper lung sextants, only 11% of these patients incurred RILT. Conversely, 11 patients exhibited primary tumor involvement in the lower lung sextants and 5 of these patients incurred RILT. Through a multivariable logistic regression model that included normal lung volume, V_{20}, ADL, and V or Q iV_{20}, ADL was the most prominently associated with RILT incidence within the global lungs and contralateral lung (Table 1). However, Q and V iV_{20} were found to be the most correlated with RILT in the ipsilateral lung.

To better understand the interplay between Q and V functional distributions within the lung and its effect on RILT risk, combined V/Q metrics were quantified and analyzed, as shown in Table E3. To be considered for a combined V/Q categorization, a voxel must have the same functional classification for Q as for V. In total, an average of 77% of voxels were found to have overlapping Q and V functional categorizations, with moderate dice similarity coefficients (DSC; measure of spatial overlap) in the LF and F regions. Poor overlap was found in the HF region. Mismatched defect categorizations were also defined but did not appear to be significant in terms of RILT incidence on univariable analysis. The DSC for the LF lung was statistically significant in the global and ipsilateral lungs, and the DSC for the F lung was negatively correlated. Using combined V/Q categorizations, both LF V/Q and F V/Q were found to correlate with RILT incidence, whereas HF V/Q was not significantly associated. However, the F V/Q odds ratio <1 suggests that patients with less F V/Q are at a higher risk for RILT.

Global and ipsilateral lung percent of LF V/Q receiving ≥20 Gy (LF V/Q_{20}) were both found to be significantly associated with RILT incidence on univariate analysis. In patients who incurred RILT, the mean percent of LF V/Q and LF V/Q_{20} in the ipsilateral lung was 32% and 17%, respectively, corresponding to an average of 161 cm^3 of combined V/Q LF lung, of which 88 cm^3 received ≥20 Gy. Conversely, the mean ipsilateral LF V/Q and LF V/Q_{20} in patients without toxicity was found to be 17% and 7%, respectively, corresponding to an average of 164 cm^3 of combined Q/V LF lung, of which 69 cm^3 received ≥20 Gy. Therefore, although the volume of the LF lung was similar, patients who incurred RILT

Table 1 Multivariable logistic regression modeling for association between dose-function metrics and radiation-induced lung toxicity

Modality	Timepoint	*n*	Structure	Metric	Odds ratio	95% Confidence interval	*P*-value
Perfusion	**Before treatment**	88	Lungs-GTV	Volume, cc	1.02−	0.50−2.01	.95
				V_{20}, %	1.05−	0.94−1.17	.39
				ADL, Gy	1.12−	1.02−1.25	**.02**
				iV_{20}, a.u.	0.08−	0.01−0.91	**.05**
			Ipsilateral lung-GTV	Volume, cc	0.85−	0.16−4.05	.84
				V_{20}, %	1.01−	0.96−1.07	.66
				ADL, Gy	1.05−	1.00−1.10	.07
				iV_{20}, a.u.	0.05−	0.00−0.69	**.03**
			Contralateral lung-GTV	Volume, cc	0.91−	0.25−2.97	.87
				V_{20}, %	1.00−	0.86−1.15	.95
				ADL, Gy	1.52−	1.06−2.23	**.03**
				iV_{20}, a.u.	0.82−	0.13−4.88	.83
Ventilation	**Before treatment**	88	Lungs-GTV	Volume, cc	1.00−	0.49−1.98	.99
				V_{20}, %	1.06−	0.95−1.19	.29
				ADL, Gy	1.14−	1.03−1.26	**.01**
				iV_{20}, a.u.	0.06−	0.00−0.64	**.02**
			Ipsilateral lung-GTV	Volume, cc	0.87−	0.17−3.99	.86
				V_{20}, %	1.02−	0.97−1.08	.39
				ADL, Gy	1.05−	1.00−1.10	.08
				iV_{20}, a.u.	0.06−	0.00−0.61	**.03**
			Contralateral lung-GTV	Volume, cc	1.47−	0.41−5.10	.54
				V_{20}, %	0.99−	0.85−1.12	.88
				ADL, Gy	1.36−	0.92−2.01	.12
				iV_{20}, a.u.	1.24−	0.15−9.27	.83

Abbreviations: ADL = average dose to the lower region of lung structure in Gy; GTV = gross tumor volume; iV_{20} = average normalized functional intensity receiving ≥20 Gy in arbitrary units; V_{20} = volume of lung structure receiving ≥20 Gy as a percent of total lung structure volume; volume = normal lung volume excluding GTV.

were delivered ≥20 Gy to an additional 19 cm^3 of LF lung on average. In a univariable ROC analysis, LF V/Q_{20} was the best predictor of RILT incidence for both the global (AUC = 0.76) and ipsilateral (AUC = 0.79) lungs compared with V_{20}, Q iV_{20}, and V iV_{20}, as shown in Table 2. Furthermore, all ipsilateral lung metrics had higher AUC values than their global lung counterparts. Based on the results of the multivariable logistic regression, LF V/Q_{20} (selected functional metric) was combined with ADL (representative locational metric) in a multivariate ROC analysis, but no additional predictive power was observed.

Despite this result, the angle of the 20% RILT risk line based on LF V/Q_{20} versus ADL in the ipsilateral lung, as shown in Figure 2, demonstrates influence from both metrics, suggesting independent vulnerabilities that lead to RILT based on the dose to the LF and the lower lung. By assigning limits of 20 Gy to lower lung and 15% LF V/Q_{20} that generally represent >20% RILT risk, there appears to be 4 RILT cases in each of the 3 labeled sections, demonstrating the independent and overlapping vulnerabilities. The full results from the multivariate models are provided in Table 3. Interestingly, both patients who incurred grade 5 RILT in this cohort presented with lower-lung tumors with an adjacent combined V/Q functional defect that received a large portion of a high dose (Fig. 3). Furthermore, although the depicted treatment planning CT scans are of limited diagnostic quality, both patients appear to exhibit significant pulmonary fibrosis before RT.

Discussion

The goal of this study was to analyze V/Q SPECT functional lung images to better understand the interplay between dose delivery and functional lung distribution with regard to RILT incidence in patients with NSCLC treated with RT. By using novel methods for the quantification of absolute functional intensity and combined V/Q functional lung categorization, patient-specific functional distributions and dose-function metrics were generated to characterize pulmonary condition and dose delivered to various functional lung regions. These methods were applied to V/Q SPECT scans from 88 patients with NSCLC accrued in 2 separate clinical trial cohorts. Through this analysis, a wide range in functional capability, including a large presence of

Table 2 Receiver operating characteristic analysis for Q, V, and combined Q/V logistic regression models to predict RILT incidence

Structure	Metric	Area under the curve	95% Confidence interval
Lungs-GTV	V_{20}, %	0.69—	0.55—0.82
	Q iV_{20}, a.u.	0.67—	0.54—0.79
	V iV_{20}, a.u.	0.68—	0.56—0.81
	Low-functioning Q + V receiving ≥20 Gy, %	0.76—	0.65—0.87
	ADL, Gy*	0.65—	0.52—0.78
	Low Q/V ≥20, %*		
Ipsilateral lung-GTV	V_{20}, %	0.74—	0.62—0.85
	Q iV_{20}, a.u.	0.7—	0.58—0.82
	V iV_{20}, a.u.	0.74—	0.63—0.85
	Low-functioning Q + V receiving ≥20 Gy, %	0.79—	0.65—0.87
	ADL, Gy*	0.75—	0.63—0.87
	Low Q/V ≥20, %*		
Contralateral lung-GTV	V_{20}, %	0.35—	0.21—0.48
	Q iV_{20}, a.u.	0.33—	0.18—0.49
	V iV_{20}, a.u.	0.34—	0.18—0.51
	Low-functioning Q + V receiving ≥20 Gy, %	0.37—	0.22—0.52
	ADL, Gy*	0.31—	0.14—0.48
	Low Q/V ≥20, %*		

Abbreviations: ADL = average dose to lower region of lung structure in Gy; GTV = gross tumor volume; iV_{20} = average normalized functional intensity receiving ≥20 Gy in arbitrary units; low Q/V ≥20 = Q/V low-function volume, defined as the intersection between low-function Q and low-function V, that received ≥20 Gy as a percent of the total lung structure volume; Q = perfusion; V = ventilation; V_{20} = volume of lung structure receiving ≥20 Gy as a percent of the total lung structure volume.

* Multivariate logistic regression model.

functional defects primarily located in the ipsilateral lung, was observed. Although the lungs are known to act as a parallel organ, NSCLC tumors are often primarily located within one lung, which can lead to a large imbalance in functional capacity between the ipsilateral and contralateral lungs. Previous work has suggested that individual lung metrics may provide deeper insight into the relationship between dose, function, and toxicity.[25]

In this study, dose-function metrics in the ipsilateral lung and ADL were found to have the highest correlation with RILT incidence. The correlation between ADL and RILT suggests a physiological radiosensitivity in the lower lung, which is consistent with previous studies that reported on the increased vulnerability of the inferior lung.[26,27,28] Moreover, ipsilateral lung Q and V mean intensity receiving ≥20 Gy were both associated with RILT. Because the estimated odds ratios for these associations were found to be less than unity, these results suggest that patients receiving ≥20 Gy to a lower average functional intensity are at an increased risk to incur RILT. To further investigate this functional sensitivity, combined V/Q metrics were generated by considering both the Q and V intensities in the voxel-wise functional categorization. Similar to the individual V/Q analysis, patients receiving ≥20 Gy to a large percentage of the combined V/Q LF lung were found to be at the highest risk for RILT.

These results were surprising based on the previous literature. Various studies have reported on the time-dependent reduction in the normal lung,[29,30] in which functional damage occurs at a higher rate in HF lungs.[31] Moreover, many studies have reported that a dose to a higher percent of functional intensity is associated with RILT.[32] Although normal lung doses should clearly be kept to a minimum to reduce functional damage, measuring the fraction of V/Q intensity receiving ≥20 Gy, in theory, only significantly differs from V_{20} in patients with heterogeneous lung function. In these cases, where total intensity (denominator of fV_{20}) is compromised relative to the rest of the cohort, the amount of functional intensity irradiated (nominator of fV_{20}) is less for a given fV_{20} value than in a patient with homogeneous lung function. Thus, fV_{20} effectively downplays the dose-effect in the LF lung. As shown in Figures E5C and D, many patients with large ipsilateral Q fV_{20} values were also delivered a high dose to a large portion of the ipsilateral LF lung.

To better quantify the interplay between the dose delivery and patient-specific functional lung distributions, the amount of each functional lung categorization delivered ≥20 Gy (LF_{20}/F_{20}/HF_{20}) was calculated as a percent of the total lung structure volume. Although the amount of LF and HF Q in the global lung was similar, LF_{20} was found to be nearly 4 times higher than HF_{20}, meaning that a high dose was more likely to be directed through LF Q

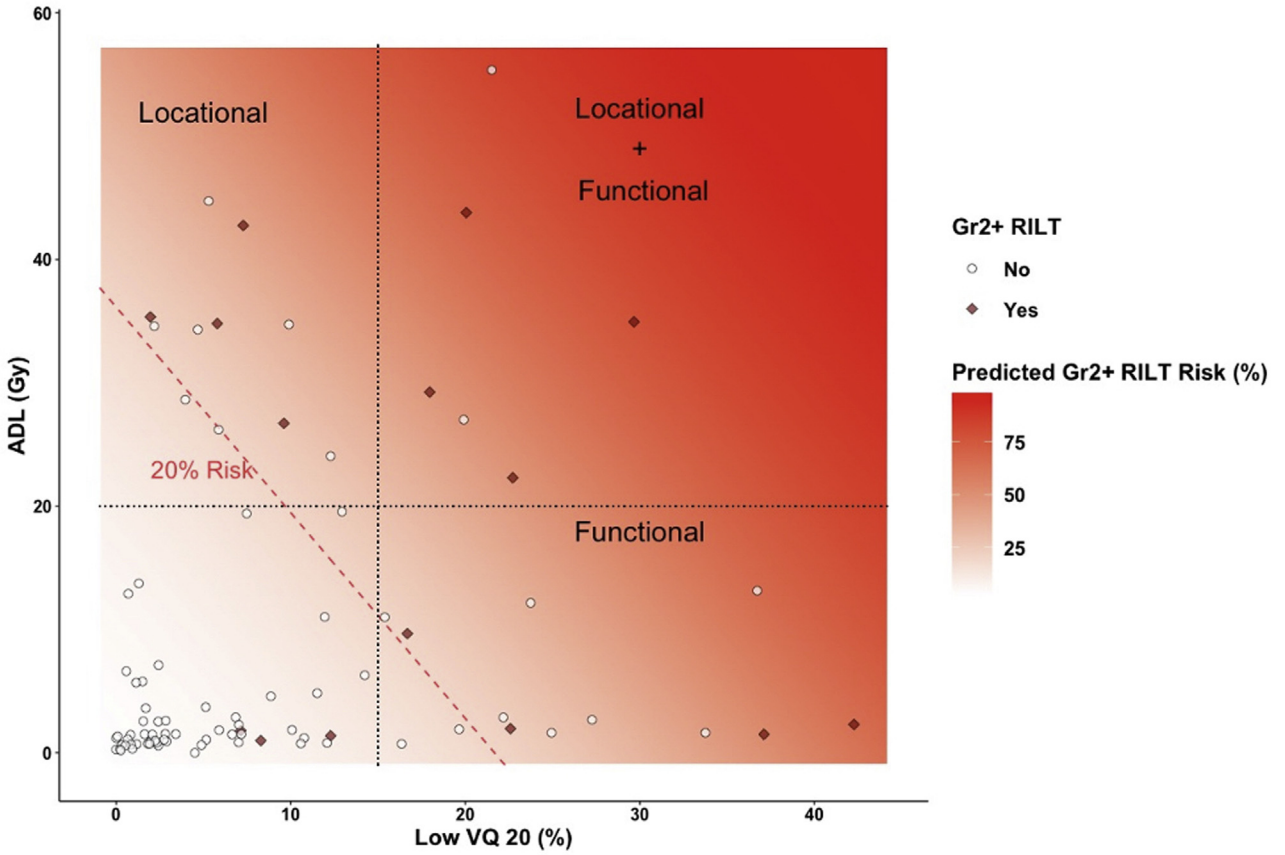

Figure 2 Scatter plot of percent of ipsilateral lung with combined perfusion/ventilation low-function receiving ≥20 Gy and average dose to lower ipsilateral lung for patients with grade 0 to 1 radiation-induced lung toxicity (RILT; white circles) versus grade 2 to 5 RILT (red diamonds). The estimated RILT risk based on logistic regression analysis is overlaid (shaded red) and the 20% risk threshold is explicitly shown (dotted red line). Independent functional (combined perfusion/ventilation low-function receiving ≥20 Gy) and locational (average dose to lower ipsilateral lung ≥20 Gy) radiation sensitivities are hypothesized based on these results. (A color version of this figure is available at https://doi.org/10.1016/j.adro.2021.100666.)

than HF Q. A higher prevalence of LF in the ipsilateral lung also suggests that the LF lung was primarily located near the tumor, whereas the HF lung was generally more concentrated in the contralateral lung. A recent study suggested that dose to 4-dimensional CT highly ventilated lung is most predictive of RP;[33] however, how well deformation-based V metrics correlate with pulmonary function is unclear. Similarly, HF lung can be hard to interpret physiologically. In terms of SPECT imaging, HF regions signify accumulated intensity that may be caused by patient geometry or saturation artifacts. The poor DSC between Q and V HF lungs found in these patients suggest that the HF regions were not well-related. Alternatively, LF and F lungs were found to have more V/Q spatial overlap and volume.

Combined V/Q functional categorizations were quantified to improve confidence in the determination of functional versus dysfunctional lung.[34] In this context, combined V/Q F and HF lungs represent regions of functional gas exchange, and combined V/Q LF lung represents regions with matching V/Q defects. Furthermore, an aggressive LF lung bound (<15% of maximum intensity) was implemented to capture the most significant defects. Although the specific cause of the functional defect is unknown, pulmonary dysfunction in these patients is primarily attributed to either tumor burden or lung disease.[35,36] Therefore, irradiating these functional defects could possibly cause a large dose to the reperfused/reventilated lung or an exacerbation of pulmonary comorbidities, which may be an explanation for the increased radiosensitivity in the LF lung found in this study.

Numerous studies have previously reported a strong connection between preexisting pulmonary comorbidities and radiation-induced lung toxicity.[37,38] Specifically, recent studies have suggested that patients with interstitial lung disease[39,40] or idiopathic pulmonary fibrosis[41,42] before RT are disproportionately prone to developing severe toxicity. Despite this known risk factor, LF lungs, which may be indicative of disease, are generally deemed less important in the dose-function response than HF lungs. However, there are indications that severe RILT is linked with a rapid progression of out-of-field

Table 3 Receiver operating characteristic analysis for combined Q/V and dose multivariate model

Structure	Metric	Odds ratio	95% confidence interval	*P*-value	Area under the curve (95% confidence interval)
Lungs-GTV	ADL, Gy	1.15−	1.05−1.27	**0.004**	0.65 (0.52−0.78)
	Low Q/V ≥20 Gy, %	1.19−	1.06−1.36	**0.006**	
Ipsilateral lung-GTV	ADL, Gy	1.06−	1.01−1.10	**0.011**	0.75 (0.63−0.87)
	Low Q/V ≥20 Gy, %	1.10−	1.04−1.17	**0.002**	
Contralateral lung-GTV	ADL, Gy	1.51−	1.06−2.17	**0.022**	0.31 (0.14−0.48)
	Low Q/V ≥20 Gy, %	0.90−	0.44−1.37	0.687	

Abbreviations: ADL = average dose to the lower region of lung structure in Gy; GTV = gross tumor volume; low Q/V ≥20 = Q/V low-function volume, defined as the intersection between low-function Q and low-function V, that received ≥20 Gy as a percent of the total lung structure volume; Q = perfusion; V = ventilation.

radiographic changes that may be indicative of a global lung immune response.[43] As stated by Makimoto et al. in 1999:[44] "Baseline impairment of pulmonary function will add to radiation damage and cause symptoms with smaller radiation volumes than in patients with normal function."[45,46]

The two grade 5 RILT cases in this study both presented with matching V/Q functional defects in the inferior region of the ipsilateral lung, appeared to exhibit pulmonary fibrosis on the treatment planning CT, and the patients ultimately died of hypoxic respiratory failure. Therefore, although further research is needed, this course of failure could be indicative of an immunologic response,[47] potentially caused by a cascade of inflammatory cytokines[48] that is initiated due to the radiation-induced exacerbation of pulmonary disease.[49] Ideally, if the presence of idiopathic pulmonary fibrosis or interstitial lung disease was clinically confirmed, these comorbidities would have been addressed or the patients would have been excluded from treatment, which demonstrates the need to screen patients with NSCLC for comorbidities before RT. Although the grade 5 RILT cases represent the most severe negative response, the pattern of irradiating large portions of LF lungs is consistently observed in RILT cases from both cohorts.

Functional-guided RT has primarily been employed to shape radiation fields to avoid functional lung and funnel dose through LF regions. A functional-avoidance technique was employed in the latter patient cohort (n = 30) to protect against irradiating above-average Q and V. Despite these included functional priorities in treatment planning, Q fV_5 was the only dose-function metric found to significantly differ between the patient cohorts, suggesting that the ability to significantly shift dose to spare functional lung was limited. Of the 8 RILT cases that received LF V/Q_{20} to >15% of the ipsilateral lung, half were from the former and half from the latter cohort, suggesting that the functional sensitivity of the LF lung was similar in each cohort despite the use of functional-avoidance RT in the latter cohort. Patients with compromised lung function before RT are generally thought to be more prone to toxicity.[50] Increased fluorodeoxyglucose-PET uptake in the normal lung (marker of pulmonary inflammation) has been shown to correlate with RP incidence,[51] especially in patients who also receive a high mean lung dose.[52] Similarly, in 2018, Otsuka et al. published a study that concluded that a high dose to poorly functioning regions, as determined by 4-dimensional CT V, was associated with the highest risk of toxicity.[53] However, dysfunctional lung sensitivity to RT has never been shown on V/Q SPECT imaging.

SPECT is a direct measure of Q or V intensity, such that combined V/Q represents functional gas exchange, and is considered the gold standard in functional lung imaging but is nonspecific for regions of dysfunction. Alternatively, normal lung PET imaging can measure pulmonary inflammation and CT can measure parenchymal density, which may be related to lung disease. Consequently, these imaging modalities are often used in the context of quantifying dysfunctional lung as opposed to SPECT, which is primarily used for functional lung quantification. As such, there has been limited investigation into the dose-effect in SPECT-based LF lung regions. Yet, because patients who benefit the most from functional-guided RT are those with functional defects, further work is needed to understand the underlying pathology of these defected regions and its effect on the biologic makeup in the lung before RT. In other words, limiting the dose to the normal lung is suggested in all cases, but identifying patients with an increased risk for severe RILT before RT should be the highest priority. Especially with concurrent immunotherapy becoming the standard of care in patients with NSCLC undergoing RT, patient-specific functional estimates are needed to identify patients with comprised lung function. Ultimately, further research is paramount to understand the immune reaction to RT such that the individual response can be optimized.[54]

Although the results of this study suggest that irradiating LF tissue plays a role in the onset of RILT, there are many challenges in the quantification of V/Q SPECT. A cleansing methodology was implemented to remove saturation artifacts, but in many cases, deciphering true functional intensity from an artifact can be difficult. Because the

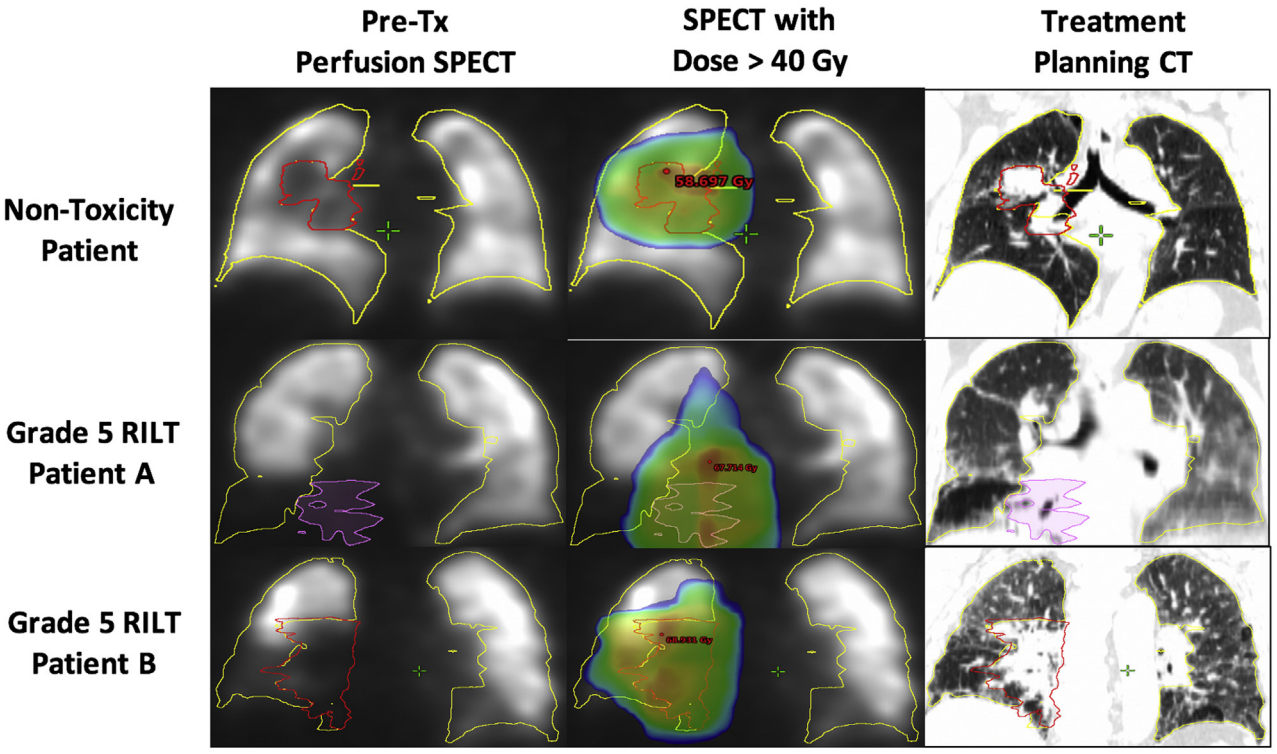

Figure 3 Pretreatment perfusion scans (left column), overlaid with dose >40 Gy (middle column), and the treatment planning computed tomography (right column) for a nontoxicity patient (top row), grade 5 Patient A (middle row), and grade 5 Patient B (bottom row).

resolution of SPECT images is limited, combined V/Q functional categorizations were implemented to represent regions with a high probability of pulmonary dysfunction but of unknown etiology. Similarly, regional lung segments and individual lung structures were used to refine the area of interest, yet better functional localization could further improve risk estimates. Functional imaging is challenging to quantify and even more challenging to compare due to the complexities of the lungs and the various imaging modalities. However, by implementing 3 functional lung categorizations (low, normal, high) and establishing an average normalized functional intensity of 1.0 for normal lungs, this study aimed to provide a template for standardization that can be expanded upon to improve our understanding of the role of irradiating functional lung in the onset of RILT.

Conclusions

This study evaluated Q, V, and combined V/Q SPECT functional metrics in 88 patients with NSCLC treated with conventionally fractionated RT. Through this analysis, patients at the highest risk for RILT were found to be those who received a high dose to the lower lung or LF regions of the ipsilateral lung at baseline. This result runs counter to the hypothesis that redistributing doses from HF to LF regions of the lung is a strategy that likely decreases toxicity. Future studies are warranted to better characterize the effect of irradiating dysfunctional lungs, and determine the appropriate role for functional image-guided treatment planning for patients with NSCLC and heterogeneously distributed lung function.

Acknowledgments

The authors gratefully acknowledge the support and collaboration of Kirk Frey MD, PhD, and colleagues at the University of Michigan, Department of Radiology for support in obtaining the protocol single-photon-emission computed tomography/computed tomography scans that were used in this work.

Supplementary Materials

Supplementary material for this article can be found at https://doi.org/10.1016/j.adro.2021.100666.

References

1. Chun SG, Hu C, Choy H, et al. Impact of intensity-modulated radiation therapy technique for locally advanced non-small-cell lung cancer: A secondary analysis of the NRG oncology RTOG 0617 randomized clinical trial. *J Clin Oncol*. 2017;35:56-62.
2. Kong (Spring) FM, Machtay M, Bradley J, et al. RTOG 1106/ACRIN 6697, randomized phase II trial of individualized

adaptive radiotherapy using during-treatment FDG-PET/CT and modern technology in locally advanced non-small cell lung cancer (NSCLC). *NRG Oncol*. 2016.
3. Boersma LJ, Damena EMF, de Boer RW, et al. A new method to determine dose-effect relations for local lung-function changes using correlated SPECT and CT data. *Radiother Oncol*. 1993;29:110-116.
4. Marks LB, Spencer DP, Bentel GC, et al. The utility of SPECT lung perfusion scans in minimizing and assessing the physiologic consequences of thoracic irradiation. *Int J Radiat Oncol Biol Phys*. 1993;26:659-668.
5. Boersma LJ, Damen EMF, de Boer RW, et al. Dose-effect relations for local functional and structural changes of the lung after irradiation for malignant lymphoma. *Radiother Oncol*. 1994;32:201-209.
6. Marks LB, Munley MT, Spencer DP, et al. Quantification of radiation-induced regional lung injury with perfusion imaging. *Int J Radiat Oncol Biol Phys*. 1997;38:399-409.
7. Marks LB, Spencer DP, Sherouse GW, et al. The role of three dimensional functional lung imaging in radiation treatment planning: The functional dose-volume histogram. *Int J Radiat Oncol Biol Phys*. 1995;33:65-75.
8. Seppenwoolde Y, Engelsman M, De Jaeger K, et al. Optimizing radiation treatment plans for lung cancer using lung perfusion information. *Radiother Oncol*. 2002;63:165-177.
9. Seppenwoolde Y, Muller SH, Theuws JC, et al. Radiation dose-effect relations and local recovery in perfusion for patients with non-small-cell lung cancer. *Int J Radiat Oncol Biol Phys*. 2000;47:681-690.
10. Vinogradskiy Y, Schubert L, Diot Q, et al. Regional lung function profiles of stage I and III lung cancer patients: An evaluation for functional avoidance radiation therapy. *Int J Radiat Oncol Biol Phys*. 2016;95:1273-1280.
11. Waxweiler T, Schubert L, Diot Q, et al. A complete 4DCT-ventilation functional avoidance virtual trial: Developing strategies for prospective clinical trials. *J Appl Clin Med Phys*. 2017;18:144-152.
12. Faught AM, Yamamoto T, Castillo R, et al. Evaluating which dose-function metrics are most critical for functional-guided radiation therapy. *Int J Radiat Oncol Biol Phys*. 2017;99:202-209.
13. Lavrenkov K, Christian JA, Partridge M, et al. A potential to reduce pulmonary toxicity: The use of perfusion SPECT with IMRT for functional lung avoidance in radiotherapy of non-small cell lung cancer. *Radiother Oncol*. 2007;83:156-162.
14. Yaremko BP, Guerrero TM, Noyola-Martinez J, et al. Reduction of normal lung irradiation in locally advanced non-small cell lung cancer patients using ventilation images for functional avoidance. *Int J Radiat Oncol Biol Phys*. 2007;68:562-571.
15. Vinogradskiy Y, Rusthoven CG, Schubert L, et al. Interim analysis of a two-institution, prospective clinical trial of 4DCT-ventilation-based functional avoidance radiation therapy. *Int J Radiat Oncol Biol Phys*. 2018;102:1357-1365.
16. Schuster J, Bayouth J. Improving pulmonary function following radiation therapy. Available at: https://clinicaltrials.gov/ct2/show/nct02843568. Accessed April 19, 2020.
17. Zeng J, Patel S, Rengan R, Bowen SR. FLARE RT for patients with stage IIB-IIIB non-small cell lung cancer: Personalizing radiation therapy using PET/CT and SPECT/CT imaging. Available at: https://clinicaltrials.gov/ct2/show/nct02773238. Accessed April 19, 2020.
18. Jolly S. Using imaging and molecular markers to predict tumor response and lung toxicity in lung cancer. Available at: https://clinicaltrials.gov/ct2/show/nct00603057. Accessed April 19, 2020.
19. Kong Spring FM, Moiseenko V, Zhao J, et al. Organs at risk considerations for thoracic stereotactic body radiation therapy: What is safe for lung parenchyma? *Int J Radiat Oncol Biol Phys*. 2018;S0360-3016:34014-34018.
20. U.S. Department of Human and Health Services. National Institutes of Health, National Cancer Institute. *Common Terminology Criteria for Adverse Events*. 4. NIH; 2009. https://ctep.cancer.gov/protocoldevelopment/electronic_applications/docs/ctcaev3.pdf. Accessed April 25, 2020.
21. Tsoutsou PG, Koukourakis MI. Radiation pneumonitis and fibrosis: Mechanisms underlying its pathogenesis and implications for future research. *Int J Radiat Oncol Biol Phys*. 2006;66:1281-1293.
22. Rubin P, Johnston CJ, Williams JP, McDonald S, Finkelstein JN. A perpetual cascade of cytokines postirradiation leads to pulmonary fibrosis. *Int J Radiat Oncol Biol Phys*. 1995;33:99-109.
23. Li AX, Alber M, Deasy JO, et al. The use and QA of biologically related models for treatment planning: short report of the TG-166 of the therapy physics committee of the AAPM. *Med Phys*. 2012;39:1386-1409.
24. Lee E, Zeng J, Miyaoka RS, et al. Functional lung avoidance and response-adaptive escalation (FLARE) RT: Multimodality plan dosimetry of a precision radiation oncology strategy. *Med Phys*. 2017;44:3418-3429.
25. Ramella S, Trodella L, Mineo C, et al. Adding ipsilateral V20 and V30 to conventional dosimetric constraints predicts radiation pneumonitis in stage IIIA-B NSCLC patients treated with combined-modality therapy. 2010;76:110-115.
26. Yorke ED, Jackson A, Rosenzweig KE, et al. Dose-volume factors contributing to the incidence of radiation pneumonitis in non-small-cell lung cancer patients treated with three-dimensional conformal radiation therapy. *Int J Radiat Oncol Biol Phys*. 2002;54:329-339.
27. Seppenwoolde Y, De Jaeger K, Boersma L, Belderbos J, Lebesque J. Regional differences in lung radiosensitivity after radiotherapy for non-small-cell lung cancer. *Int J Radiat Oncol Biol Phys*. 2004;60:748-758.
28. Bradley JD, Hope A, Naqa I El, et al. A nomogram to predict radiation pneumonitis, derived from a combined analysis of RTOG 9311 and institutional data. *Int J Radiat Oncol Biol Phys*. 2007;69:985-992.
29. Woel RT, Munley MT, Hollis D, et al. The time course of radiation therapy-induced reductions in regional perfusion: A prospective study with >5 years of follow-up. *Int J Radiat Oncol Biol Phys*. 2002;52:58-67.
30. Zhang J, Ma J, Zhou S, et al. Radiation-induced reductions in regional lung perfusion: 0.1-12 year data from a prospective clinical study. *Int J Radiat Oncol Biol Phys*. 2010;76:425-432.
31. Owen DR, Boonstra PS, Viglianti BL, et al. Modeling patient-specific dose-function response for enhanced characterization of personalized functional damage. *Int J Radiat Oncol Biol Phys*. 2018;102:1265-1275.
32. Bucknell NW, Hardcastle N, Bressel M, et al. Functional lung imaging in radiation therapy for lung cancer: A systematic review and meta-analysis. *Radiother Oncol*. 2018;129:196-208.
33. O'Reilly S, Jain V, Huang Q, et al. Dose to highly functional ventilation zones improves prediction of radiation pneumonitis for proton and photon lung cancer radiation therapy. *Int J Radiat Oncol Biol Phys*. 2020;107:79-87.
34. Yuan ST, Frey KA, Gross MD, et al. Semiquantification and classification of local pulmonary function by V/Q single photon emission computed tomography in patients with non-small cell lung cancer: Potential indication for radiotherapy planning. *J Thorac Oncol*. 2011;6:71-78.
35. Strickland NH, Hughes JM, Hart DA, Myers MJ, Lavender JP. Cause of regional ventilation-perfusion mismatching in patients with idiopathic pulmonary fibrosis: A combined CT and scintigraphic study. *AJR Am J Roentgenol*. 1993;161:719-725.
36. Bajc M, Chen Y, Wang J, et al. Identifying the heterogeneity of COPD by V/P SPECT: A new tool for improving the diagnosis of parenchymal defects and grading the severity of small airways disease. *Int J Chron Obstruct Pulmon Dis*. 2017;12:1579-1587.
37. Appelt AL, Vogelius IR, Farr KP, Khalil AA, Bentzen SM, Bentzen M. Towards individualized dose constraints: Adjusting the QUANTEC radiation pneumonitis model for clinical risk factors towards individualized dose constraints: Adjusting the QUantec

radiation pneumonitis model for clinical risk factors. *Acta Oncol*. 2014;53:605-612.
38. Kong FS, Wang S. Nondosimetric risk factors for radiation-Induced lung toxicity. *Semin Radiat Oncol*. 2015;25:100-109.
39. Ozawa Y, Abe T, Omae M, et al. Impact of preexisting interstitial lung disease on acute, extensive radiation pneumonitis: Retrospective analysis of patients with lung cancer. *PloS One*. 2015;10: e0140437.
40. Bahig H, Filion E, Vu T, et al. Severe radiation pneumonitis after lung stereotactic ablative radiation therapy in patients with interstitial lung disease. *Pract Radiat Oncol*. 2016;6:367-374.
41. Gelblum D, Rimner A, Wu AJ, Colemann A. Treatment toxicity from lung radiation therapy in patients with underlying idiopathic pulmonary fibrosis. *Int J Radiat Oncol Biol Phys*. 2015;93:E442.
42. Han SY, Lee YJ, Park JS, et al. Prognosis of non-small-cell lung cancer in patients with idiopathic pulmonary fibrosis. *Nat Sci Rep*. 2019;9:12561.
43. Keffer S, Guy CL, Weiss E. Fatal radiation pneumonitis: Literature review and case series. *Adv Radiat Oncol*. 2020;5:238-249.
44. Makimoto T, Tsuchiya S, Hayakawa K, Saitoh R, Mori M. Risk factors for severe radiation pneumonitis in lung cancer. *Jpn J Clin Oncol*. 1999;29:192-197.
45. Phillips TL. Radiation fibrosis. In: Fishman AP, ed. *Pulmonary Diseases and Disorders*. 1. New York, NY: McGraw-Hill; 1988: 773-792.
46. Monson JM, Stark P, Reilly JJ, et al. Clinical radiation pneumonitis and radiographic changes after thoracic radiation therapy for lung carcinoma. *Cancer*. 1998;82:842-850.
47. Moodley YP, Misso NLA, Scaffidi AK, et al. Inverse effects of interleukin-6 on apoptosis of fibroblasts from pulmonary fibrosis and normal lungs. *Am J Resp Cell Mol Biol*. 2003;29:490-498.
48. Siva S, MacManus M, Kron T, et al. A pattern of early radiation-induced inflammatory cytokine expression is associated with lung toxicity in patients with non-small cell lung cancer. *PloS One*. 2014; 9:e109560.
49. Kim H, Yoo H, Pyo H, et al. Impact of underlying pulmonary diseases on treatment outcomes in early-stage non-small cell lung cancer treated with definitive radiotherapy. *Int J Chron Obstruct Pulmon Dis*. 2019;14:2273-2281.
50. Abratt RP, Morgan GW. Lung toxicity following chest irradiation in patients with lung cancer. *Lung Cancer*. 2002;35:103-109.
51. Castillo R, Pham N, Ansari S, et al. Pre-radiotherapy FDG PET predicts radiation pneumonitis in lung cancer. *Radiat Oncol*. 2014;9:74.
52. Chaudhuri AA, Binkley MS, Rigdon J, et al. Pre-treatment non-target lung FDG-PET uptake predicts symptomatic radiation pneumonitis following stereotactic ablative radiotherapy (SABR) pre-treatment non-target lung FDG-PET uptake predicts radiation pneumonitis after SABR. *Radiother Oncol*. 2016;119:454-460.
53. Otsuka M, Monzen H, Matsumoto K, et al. Evaluation of lung toxicity risk with computed tomography ventilation image for thoracic cancer patients. Zhang Q, ed. *PLoS One*. 2018;13: e0204721.
54. Tsoutsou PG. The interplay between radiation and the immune system in the field of post-radical pneumonitis and fibrosis and why it is important to understand it. *Exp Opin Pharmacother*. 2014;15: 1781-1783.